

## Supplementary information

### **CO<sub>2</sub>(aq) concentration–dependent CO<sub>2</sub> fixation via carboxylation by decarboxylase**

Yan Fan<sup>a,b</sup>, Jianqiang Feng<sup>c</sup>, Miao Yang<sup>a</sup>, Xin Tan<sup>d</sup>, Hongjun Fan<sup>a</sup>,

MeiJin Guo<sup>e</sup>, Binju Wang<sup>c</sup>, Song Xue<sup>\*f</sup>

<sup>a</sup> Department of Biotechnology, Dalian Institute of Chemical Physics, Chinese Academy of Sciences, 116023 Dalian, China

<sup>b</sup> University of Chinese Academy of Sciences, 100049 Beijing, China

<sup>c</sup> Department of Chemical biology, Xiamen University, 361005 Xiamen, China

<sup>d</sup> National Center of Bio-Engineering & Technology, 201499 Shanghai, China

<sup>e</sup> School of Biotechnology, East China University of Science and Technology, 200237 Shanghai, China

<sup>f</sup> School of Bioengineering, Dalian University of Technology, 116024 Dalian, China

\*correspondence to: [xuesong@dlut.edu.cn](mailto:xuesong@dlut.edu.cn), Tel.: 13898626890

### Table of contents

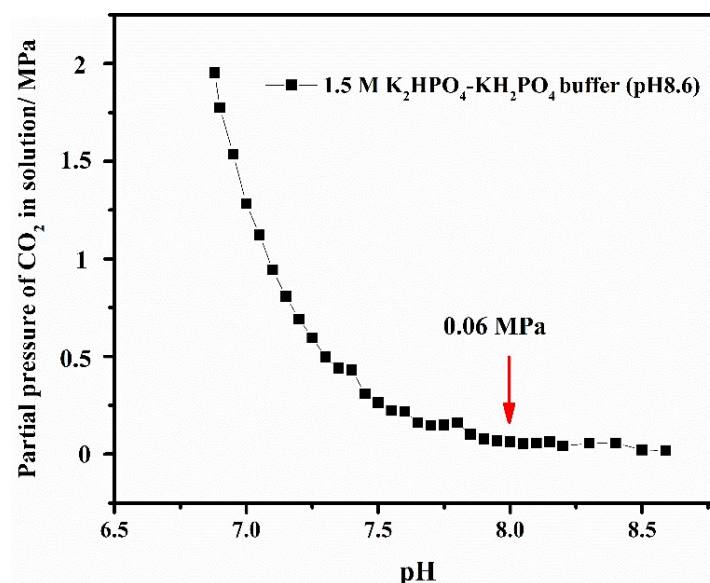
1. Calculation of energy barrier of different substrates	2
2. <b>Figure S.1.</b>	3
3. <b>Figure S.2.</b>	3
4. <b>Figure S.3.</b>	4
5. <b>Figure S.4.</b>	5
6. <b>Table S.1.</b>	5
7. <b>Table S.2.</b>	5
8. <b>Table S.3.</b>	5
9. <b>References</b>	6

## Calculation of energy barrier of different substrates

**System setup.** The initial structure of 2,3-DHBD\_Ao was prepared from its crystal structure, by which  $\text{CO}_2$  and  $\text{HCO}_3^-$  was manually added to the active site. The protonation states of titratable residues (His, Glu, and Asp) were assigned based on their pKa values obtained from PROPKA software, as well as on their local hydrogen bonds. His167, His200, His222 and His236 were protonated at the  $\delta$  position, and His34, His48, His52, His106, His195, His213, His226 and His270 were protonated at the  $\epsilon$  position. All glutamic acid and aspartic acid residues were deprotonated. The force field parameters were set using the “MCPB.py” modeling tool<sup>1, 2</sup> available in AmberTools18. All amino acid residues were applied with the Amber ff14SB force field,<sup>3</sup> whereas the substrates and co-substrates were applied with the general AMBER force field (GAFF).<sup>4</sup> The partial atomic charges were obtained by the RESP method.<sup>5</sup> Missing parameters for the substrates and co-substrates were generated by the parmchk utility available in AmberTools18. Sodium ions were added to the protein surface to neutralize the total charge of the system. Finally, the system was solvated in a rectangular box of TIP3P waters with a size extending up to a distance of at least 16 Å from the protein surface.

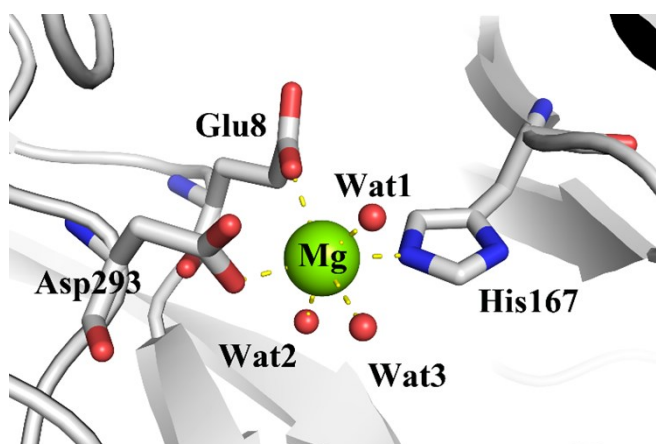
**QM model calculations.** All QM model calculations were performed by Gaussian 09 software. The geometries of the species of interest were fully optimized in conjunction with the SMD<sup>6</sup> continuum solvation model at the B3LYP-D3/def2-SVP level of theory. For Mg(II)-substrate, the calculations were completed in the singlet spin state. For the reactivity of conformation, the QM region was set to contain metal, catechol substrate,  $\text{CO}_2/\text{HCO}_3^-$  co-substrate, and water (to maintain the coordination number of the metal), as well as amino acids Glu8, His167 and Asp293, which were coordinated with the metals.

**QM/MM calculations.** All QM/MM calculations for the QM region were performed using ChemShell<sup>7, 8</sup> combined with Turbomole<sup>9</sup> and those for the MM region were performed using DL\_POLY.<sup>10</sup> The electronic embedding scheme was used to determine the polarizing effect of the enzyme environment on the QM region.<sup>11</sup> The QM/MM boundary was treated with the hydrogen link atoms using the charge-shift model.<sup>8</sup> In QM/MM geometry optimizations, the QM region was defined by the hybrid B3LYP density functional with the def2-SVP levels of theory. Dispersion corrections by the Grimme’s D3(BJ) method<sup>12-14</sup> were included in all QM/MM calculations. The QM region was set to consist of Mg cofactor,  $\text{CO}_2$ ,  $\text{H}_2\text{O}$ , 2,3-DHBD (the substrate), and the sidechains of Glu8, His167, His222, and Asp293. All the transition states (TSs) were located using relaxed potential energy surface (PES) scans, followed by full TS optimizations using the dimer optimizer available in the DL-FIND code.<sup>15</sup>



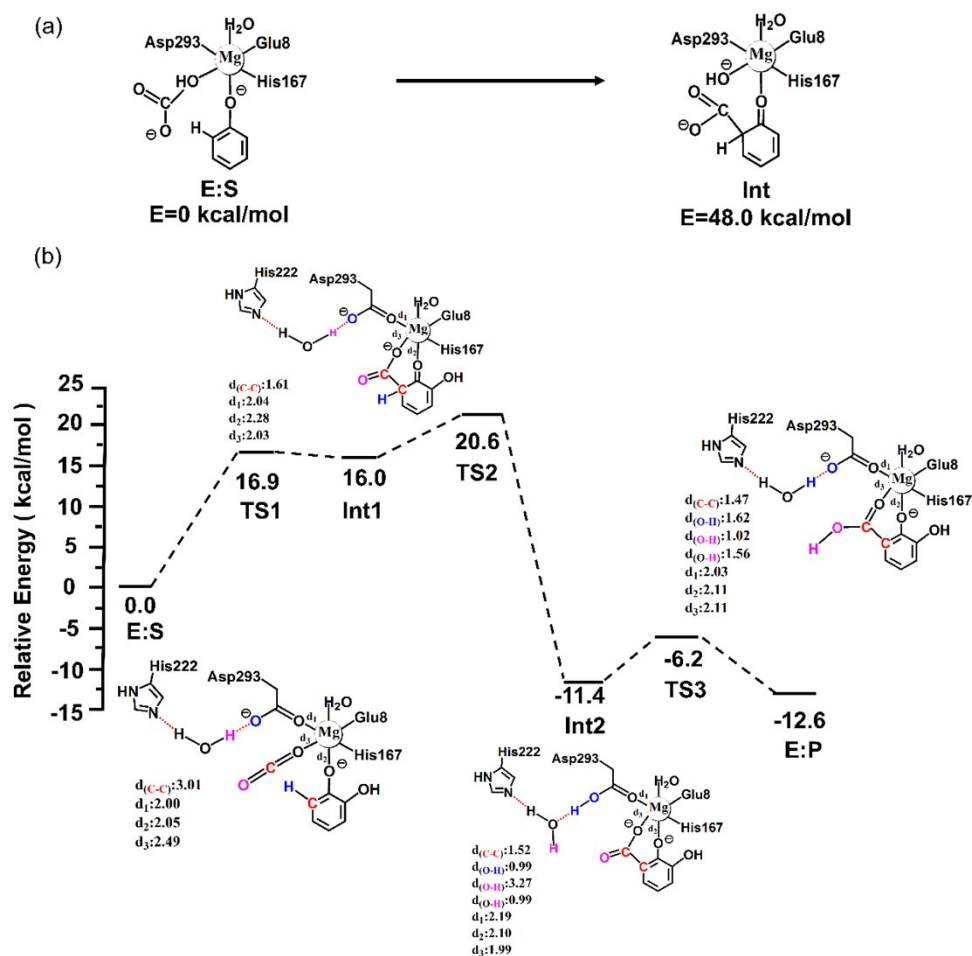
**Figure S.1.** The pH and the corresponding CO<sub>2</sub> partial pressure in the 1.5 M K<sub>2</sub>HPO<sub>4</sub>-KH<sub>2</sub>PO<sub>4</sub> buffer (pH8.6) with 0.2 MPa CO<sub>2</sub>

Figure S.1 shows that in K<sub>2</sub>HPO<sub>4</sub>-KH<sub>2</sub>PO<sub>4</sub> buffer containing 0.02 MPa CO<sub>2</sub>, the CO<sub>2</sub> partial pressure was only 0.06 MPa when pH was higher than 8.0, and the yield was only 6.2%.



**Figure S.2** Coordination of Mg<sup>2+</sup> in the active center of 2,3-DHBD\_Ao

Figure S.2 shows that the crystal of 2,3-DHBD\_Ao. It was obtained under the reservoir condition containing 0.2 M Sodium Chloride, 0.1M Bis-Tris pH5.5, 25%w/v PEG 3350. Crystals grew to a maximal size at room temperature in 3-5 days, which reached dimensions suitable for X-ray diffraction. 2,3-DHBD\_Ao structure was determined by molecular replacement using structure of 2,6-DHBD (PDB code 2DVT) as an initial search model. The water was shown in red sphere, the metal ion was shown in green sphere. Wat: water.



**Figure S.3.** Identification of carboxylate donor by energy barrier calculation. (a) Calculated energy barrier for  $\text{HCO}_3^-$  as a carboxylation substrate. (b) Calculated energy profiles for  $\text{CO}_2$  as a carboxylation substrate.

Figure S.3(a) shows that 48 kcal/mol was required for the formation of intermediate (**Int**) when  $\text{HCO}_3^-$  as the carboxylate donor.

Figure S.3(b) shows that the enzyme-product complex (E:P) is calculated to be 12.6 kcal/mol lower than the enzyme-substrate (E:S). The first step is calculated to have a barrier of 16.9 kcal/mol, and the resulting the intermediate **Int1** is 16.0 kcal/mol higher than the enzyme-substrate (E:S). The second step is calculated to be rate-limiting with a barrier of 20.6 kcal/mol. The resulting intermediate **Int2** is 11.4 kcal/mol lower in energy than the enzyme-substrate (E:S). From here, a proton transfer from  $\text{H}_2\text{O}$  to 2,3-DHBA take place, with a calculated barrier of 5.4 kcal/mol.

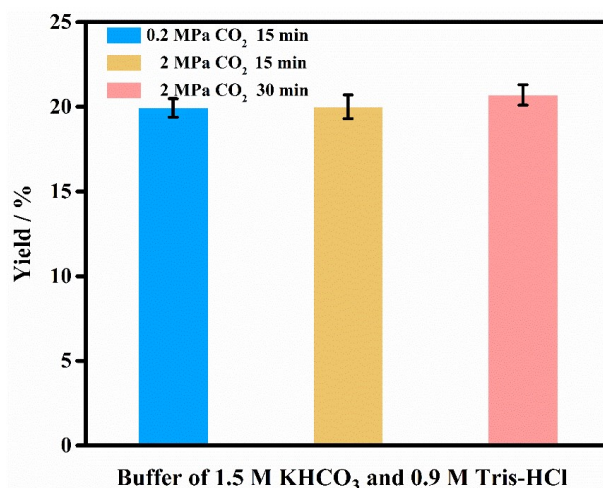


**Figure S.4.** Carboxylation efficiency under the combination of 1.5 M KHCO<sub>3</sub> and 0.9 M Tris-HCl buffer

**Table S.1.** Determination of active center metal ions in 2,3-DHBD\_Ao by ICP-OES

Metal ion	C(Enzyme)/C(Metal ion)
Mg	1
Ca	13
Zn	78
Mn	30

The metal ion concentrations of a certain amount of protein were determined by ICP-OES. The concentrations of calcium, magnesium, zinc, and manganese ions in the protein were measured. The metal ion of the protein was determined by whether the ration between the content of the metal ion and the target protein were 1:1.

**Table S.2.** Carboxylation efficiency in 2.2 M KHCO<sub>3</sub> at 4°C

Reaction time / min	Yield / %
15	21.8 ± 0.2
60	26.1 ± 0.2

**Table S.3.** The calculation and comparison of TOF

Enzyme	Substrate	TOF/min <sup>-1</sup>
Fo_2,3-DHBD	Catechol	0.03 <sup>16</sup>
Ao_2,3-DHBD	resorcinol	0.23 <sup>17</sup>
Ao_2,3-DHBD	Catechol	47

The “turnover frequency” (TOF) is defined as “molecules reacting per active site per time” to measure the instantaneous efficiency of a catalyst.<sup>18</sup>

## References

1. P. Li and K. M. J. Merz, *J. Chem. Inf. Model.*, 2016, 56, 599-604.
2. P. Li and K. M. J. Merz, *Chem. Rev.*, 2017, 117, 1564-1686.
3. J. A. Maier, C. Martinez, K. Kasavajhala, L. Wickstrom, K. E. Hauser and C. Simmerling, *J. Chem. Theory. Comput.*, 2015, 11, 3696-3713.
4. J. M. Wang, R. M. Wolf, J. W. Caldwell, P. A. Kollman and D. A. Case, *J. Comput. Chem.*, 2004, 25, 1157-1174.
5. C. I. Bayly, P. Cieplak, W. D. Cornell and P. A. Kollman, *J. Phys. Chem.*, 1993, 97, 10269-10280.
6. A. V. Marenich, C. J. Cramer and D. G. Truhlar, *J. Phys. Chem. B.*, 2009, 113, 6378-6396.
7. S. Metz, J. Kästner, A. A. Sokol, T. W. Keal and P. Sherwood, *Wires. Comput. Mol. Sci.*, 2013, 4, 101-110.
8. A. H. de Vries, P. Sherwood, S. J. Collins, A. M. Rigby, M. Rigutto and G. J. Kramer, *J. Phys. Chem. B.*, 1999, 103, 6133-6141.
9. R. Ahlrichs, M. Bär, M. Häser, H. Horn and C. Kölmel, *Chem. Phys. Lett.*, 1989, 162, 165-169.
10. W. Smith, C. W. Yong and P. M. Rodger, *Mol. Simulat.*, 2002, 28, 385-471.
11. D. Bakowies and W. Thiel, *J. Phys. Chem.*, 1996, 100, 10580-10594.
12. S. Grimme, *J. Comput. Chem.*, 2006, 27, 1787-1799.
13. S. Grimme, J. Antony, S. Ehrlich and H. Krieg, *J. Chem. Phys.*, 2010, 132, 154104.
14. S. Grimme, S. Ehrlich and L. Goerigk, *J. Comput. Chem.*, 2011, 32, 1456-1465.
15. J. Kästner, J. M. Carr, T. W. Keal, W. Thiel, A. Wander and P. Sherwood, *J. Phys. Chem. A.*, 2009, 113, 11856-11865.
16. X. Zhang, J. Ren, P.-Y. Y, R. Gong, M. Wang, Q.-Q. Wu and D.-M. Zhu, *Enzyme Microb. Technol.*, 2018, 113, 37-43.
17. K. Plasch, G. Hofer, W. Keller, S. Hay, D. J. Heyes, A. Dennig, S. M. Glueck and K. Faber, *Green Chem.*, 2018, 20, 1754-1759.
18. S. Kozuch and J. M. L. Martin, *ACS Catal.*, 2012, 2, 2787-2794.